Frontiers in Bioscience Landmark

Front. Biosci. (Landmark Ed) **2026**; 31(6): 50007
https://doi.org/10.31083/FBL50007

Original Research

Multi-Method Investigation of the Role of the PI3K/Akt Pathway in Sinomenine-Mediated Neuroprotection Against Acute Ischemic Stroke

Xinzuo Qin[1], Wancheng Zheng[1], Xiaoqun Li[2], Yun Du[1], Lulu Wen[1], Miao Qu[1,*]

[1]Department of Neurology, Xuanwu Hospital, Capital Medical University, 100053 Beijing, China
[2]Department of Encephalopathy, Third Clinical Medical College of Beijing University of Chinese Medicine, 100029 Beijing, China
*Correspondence: qumiao@xwhosp.org (Miao Qu)

Academic Editors: Moo-Ho Won and Thomas Heinbockel
Submitted: 14 January 2026 Revised: 29 April 2026 Accepted: 11 May 2026 Published: 25 June 2026

Abstract

Background: Effective neuroprotective therapies for acute ischemic stroke (AIS) remain limited due to the complex interplay between neuroinflammation and apoptosis. Sinomenine (Sino), a bioactive alkaloid derived from Sinomenium acutum, exhibits anti-inflammatory and anti-apoptotic activities; however, its molecular targets and mechanisms in AIS remain unclear. This study aimed to identify potential targets and key pathways of Sino and validate its neuroprotective effects in AIS. **Methods**: A combined approach integrating network pharmacology, Mendelian randomization (MR), molecular docking, and *in vivo* validation was adopted. Potential targets of Sino and ischemic stroke were identified using public databases. Overlapping targets were analyzed through protein-protein interaction network construction and Gene Ontology (GO) and Kyoto Encyclopedia of Genes and Genomes (KEGG) enrichment analyses. Sprague-Dawley rats were randomly assigned to four groups, and a middle cerebral artery occlusion/reperfusion (MCAO/R) model was established (n = 12 per group): Sham, MCAO/R, Sino (20 mg/kg), and Sino +LY294002 (LY, 10 mg/kg). Sino and Sino + LY were administered intraperitoneally within 6 h after surgery and once daily thereafter for three days. Sham and MCAO groups were given the same amount of physiological saline undergoing the same procedures. Sino was administered intraperitoneally within 6 h after surgery and once daily thereafter for three days. Neurological deficits, infarct volume, neuronal injury, apoptosis, activation of the phosphatidylinositol 3-kinase/protein kinase B (PI3K/Akt) pathway, and inflammatory responses were assessed using behavioral tests, 2,3,5-Triphenyltetrazolium chloride (TTC)/Nissl/Terminal deoxynucleotidyl transferase dUTP Nick End Labeling (TUNEL) staining, Western blotting, immunofluorescence, enzyme-linked immunosorbent assay (ELISA). **Results**: Twelve overlapping targets between Sino and ischemic stroke were identified, with Akt1 recognized as a central hub. Enrichment analysis highlighted the PI3K/Akt pathway as a critical signaling axis, while MR analysis indicated a nominal association between Akt1 and ischemic stroke. Molecular docking predicted stable binding between Sino and Akt1. In MCAO/R rats, Sino significantly improved neurological function, reduced infarct volumes, attenuated neuronal apoptosis, and increased neuronal survival. Mechanistically, Sino increased the p-PI3K/PI3K and p-Akt/Akt ratios, upregulated Bcl-2 expression, and decreased the expression of Bax, cleaved caspase-3, ionized calcium-binding adapter molecule 1 (Iba1), inducible nitric oxide synthase (iNOS), interleukin-1β (IL-1β), interleukin-6 (IL-6), and tumor necrosis factor-α (TNF-α). These beneficial effects were notably attenuated by LY. **Conclusion**: This study establishes PI3K/Akt as a functionally necessary mediator of Sino's neuroprotection against cerebral ischemia/reperfusion injury. The incomplete LY reversal indicates multi-target activity, supporting Sino's development as an adjunctive therapeutic candidate for ischemic stroke.

Keywords: Sinomenine; brain ischemia; phosphatidylinositol 3-kinases; signal transduction; neuroinflammation; apoptosis

1. Introduction

Ischemic stroke remains a leading cause of mortality and long-term disability worldwide, imposing substantial socioeconomic burdens on healthcare systems [1]. Despite advances in thrombolytic therapy and endovascular thrombectomy, their narrow therapeutic windows and hemorrhagic complications limit clinical applicability. Consequently, a significant proportion of patients lack effective treatment options [2]. Therefore, there is an urgent clinical need to develop neuroprotective strategies targeting secondary brain injury following ischemia. Cerebral ischemia–reperfusion injury is a highly complex pathophysiological process involving the spatiotemporal orchestration of multiple molecular events. Although reperfusion is essential for salvaging ischemic brain tissue by restoring oxygen and nutrient supply, it can paradoxically exacerbate secondary brain injury through a series of detrimental biochemical and cellular cascades. These events are characterized by excessive oxidative stress, overwhelming inflammatory responses, apoptosis, and blood–brain barrier disruption, which collectively contribute to irreversible neuronal injury and cell death. Following cerebral ischemia, neuronal damage arises not only from the initial reduction in cerebral blood flow but also from subsequent pathological processes, among which neuroinflammation and apoptosis are central and closely interconnected mechanisms [3]. Excessive inflammatory activation and programmed cell death synergistically exacerbate blood–brain barrier disruption,

mitochondrial dysfunction, and progressive neuronal loss [4,5]. Increasing evidence suggests inflammatory signaling amplifies apoptotic cascades, while apoptosis-related mitochondrial dysfunction further fuels inflammatory responses, indicating these processes form an interdependent pathological network rather than separate events [3].

The phosphatidylinositol 3-kinase/protein kinase B (PI3K/Akt) signaling pathway has emerged as a crucial regulator linking neuronal survival, inflammation, and apoptosis following ischemic stroke [6]. Activation of PI3K/Akt signaling promotes cell survival by inhibiting pro-apoptotic mediators such as glycogen synthase kinase-3β, Bax translocation, and caspase-9 activation, thereby attenuating mitochondria-dependent apoptosis [7]. Additionally, PI3K/Akt signaling negatively regulates neuroinflammation by modulating the nuclear factor-κB (NF-κB) pathway, a central transcriptional regulator of pro-inflammatory cytokines such as IL-1β, IL-6, and TNF-α [8]. Emerging evidence supports a critical role for the PI3K/Akt signaling axis in regulating neuroinflammatory responses and cell fate determination after stroke [9]. However, pharmacological agents capable of effectively targeting the PI3K/Akt pathway to concurrently suppress inflammation and apoptosis in ischemic stroke remain scarce.

Natural products have become valuable sources for developing neuroprotective drugs due to their multi-target profiles and favorable safety characteristics [10,11]. Sinomenine (Sino), a bioactive alkaloid isolated from Sinomenium acutum, exhibits significant anti-inflammatory and anti-apoptotic effects in various neurological disorders, including cerebral ischemia [12]. Previous studies have demonstrated that Sino alleviates neuroinflammation by modulating microglial polarization and suppressing the release of pro-inflammatory cytokines [13]. However, most prior research has focused on isolated inflammatory or apoptotic outcomes without systematically exploring upstream signaling mechanisms, particularly the involvement of the PI3K/Akt pathway.

This study systematically investigates the neuroprotective effects of Sino against acute ischemic stroke (AIS) and elucidates its underlying molecular mechanisms. By integrating network pharmacology (NP), Mendelian randomization (MR), molecular docking, and *in vivo* validation using a rat middle cerebral artery occlusion/reperfusion (MCAO/R), we aimed to identify potential therapeutic targets and key signaling pathways of Sino. Additionally, we evaluated the effects of Sino on neurological deficits, cerebral infarction, neuronal injury, apoptosis, and neuroinflammation. The involvement of PI3K/Akt signaling was validated pharmacologically using the PI3K inhibitor LY294002 (LY). Collectively, this study provides mechanistic insights into the neuroprotective actions of Sino, supporting its therapeutic potential for ischemic stroke.

2. Materials and Methods

2.1 Network Pharmacology Analysis

Potential targets of Sino were identified from the TCMSP, SwissTargetPrediction (version 2021, University of Geneva, Geneva, Switzerland), and PharmMapper databases. Targets associated with ischemic stroke were retrieved from GeneCards, OMIM, and DrugBank. Overlapping targets were determined via Venn analysis. A protein-protein interaction (PPI) network was constructed using the STRING database (medium confidence ≥0.4) and visualized with Cytoscape. Gene Ontology (GO) and Kyoto Encyclopedia of Genes and Genomes (KEGG) pathway enrichment analyses were conducted using the DAVID platform. Molecular docking between Sino and key targets was performed using AutoDock Vina.

2.2 MR Analysis

Two-sample MR was conducted for the 12 candidate targets identified via NP analysis. cis-eQTLs from the eQTLGen consortium were selected as instrumental variables, and ischemic stroke GWAS data (ebi-a-GCST90018864) served as the outcome dataset. All instrumental variables satisfied genome-wide significance and independence criteria (F-statistics >10). MR analyses were performed using inverse variance weighted (IVW), weighted median, weighted mode, and MR-Egger methods. Sensitivity analyses included Cochran's Q test, MR-Egger intercept test, and leave-one-out analysis.

2.3 Animals and Experimental Design

Male Sprague–Dawley rats (250-280 g) were purchased from Beijing Viton Lever Laboratory Animal Technology Co., Ltd. (Beijing, China). Animals were housed in standard polypropylene cages (5 rats per cage, 30 cm × 20 cm × 15 cm) under controlled environmental conditions with a 12:12 h light-dark cycle, ambient temperature of 22 ± 2 °C, and relative humidity of 50–60%. All rats were acclimatized to the laboratory environment for 7 days prior to the experimental procedures, with free access to standard rodent chow and water ad libitum. All experimental procedures were approved by the Institutional Animal Care and Use Committee of Capital Medical University (approval No. AEEI-2024-129) and complied with the ARRIVE guidelines. Sino and LY were obtained from Beijing Honghu United Chemical Products Co., Ltd. (Beijing, China). Compounds were initially dissolved in dimethyl sulfoxide (DMSO) and subsequently diluted with sterile normal saline to achieve the required concentrations. The final concentration of DMSO was minimal and identical across all treatment groups.

A total of 60 rats were initially allocated across the four experimental groups. In the Sham group, all 12 animals survived the entire protocol without incident, yielding a final sample size of 12. The MCAO group began with

16 rats; however, 3 animals succumbed to surgery-related complications within 24 h postoperatively, and 1 additional rat was excluded due to unsuccessful model induction (neurological score = 0), resulting in 12 rats for final analysis. For the Sino group, 2 deaths occurred during the perioperative period, and 1 animal was excluded because of severe subarachnoid hemorrhage detected at necropsy, leaving 12 rats. In the Sino + LY group, 1 rat died following surgery, and 1 was removed from the study due to catheter displacement; the remaining 12 animals completed the protocol and were included in the statistical analysis. Rats were randomly assigned to four groups (n = 12 per group): Sham, MCAO/R, Sino (20 mg/kg), and Sino + LY (10 mg/kg). The Sino dose (20 mg/kg) was chosen based on previous reports demonstrating its neuroprotective efficacy in experimental rodent stroke models [14,15]. Sino was administered intraperitoneally starting within 6 hours post-surgery, followed by daily injections for 3 consecutive days. Medication administration and tissue collection followed a predefined protocol. Behavioral assessments were conducted by investigators blinded to group allocation. At the designated endpoint (3 days post-intervention), rats were euthanized under deep anesthesia by intraperitoneal injection of sodium pentobarbital (150 mg/kg, dissolved in sterile saline at 3% w/v). Brain tissues were rapidly dissected for subsequent analyses. Cortical tissues from the ischemic penumbra of the left hemisphere were carefully isolated and prepared for biochemical and histological analyses.

Inclusion Criteria Rats were eligible for enrollment if they met all of the following conditions: (1) clinically healthy with normal body weight and no evidence of respiratory distress, infection, or other systemic illness; (2) successful induction of focal cerebral ischemia confirmed by neurological assessment using the Longa scale (scores 1–3 were considered indicative of adequate MCAO model establishment); and (3) successful completion of the full experimental protocol without intraoperative or perioperative complications. Exclusion Criteria Animals were removed from the final dataset if any of the following occurred: (1) mortality during the surgical procedure or within the first 24 h postoperatively; (2) unsuccessful ischemia induction, defined as a neurological score of 0 (no deficit) or 4 (moribund status); (3) gross subarachnoid hemorrhage detected at necropsy; (4) complete neurological recovery to a score of 0 prior to the scheduled endpoint; or (5) protocol discontinuation due to technical issues such as catheter displacement or equipment malfunction.

2.4 Construction of the MCAO/R Model

Focal cerebral ischemia was induced using the intraluminal filament method. Rats were anesthetized with isoflurane inhalation (induction: 3–4%; maintenance: 1.5–2.0%). A nylon monofilament was inserted through the internal carotid artery to occlude the middle cerebral artery for 90 min, followed by reperfusion [16]. Sham-operated rats underwent identical surgical procedures without arterial occlusion.

2.5 Neurological Function Assessment

Neurological deficits were evaluated 3 days after surgery using the Zea-Longa, Bederson, and modified Garcia scoring systems. Two independent investigators, blinded to group allocation, conducted these assessments [17,18,19]. Discrepancies were resolved by consensus.

2.6 TTC Staining

Brains were rapidly harvested after decapitation, chilled in ice-cold saline for 5 min, and sectioned coronally into five 2-mm slices using a brain matrix. Sections were stained with 2% TTC solution (Sigma-Aldrich) for 30 min at 37 °C in the dark with gentle agitation and then fixed overnight in 4% paraformaldehyde at 4 °C. Images were captured using a stereomicroscope equipped with a digital camera under uniform illumination. A blinded investigator quantified infarct and contralateral hemisphere areas using ImageJ software (NIH). Infarct volumes were corrected for edema using the formula: infarct volume (%) = [(total infarct area × slice thickness) / (total contralateral area × slice thickness)] × 100%.

2.7 Histology and Immunofluorescence

Brain tissues from the ischemic penumbra were fixed in 4% paraformaldehyde at 4 °C for 24 h, dehydrated in graded ethanol solutions, paraffin-embedded, and sectioned coronally at 5 µm thickness (Leica RM2235).

The TUNEL assay (Roche #11684795910) was performed as follows: sections were permeabilized in 0.1% Triton X-100 for 15 min, incubated with TUNEL reaction mix (50 µL/section) at 37 °C for 60 min, and counterstained with DAPI (1 µg/mL). DNase I-treated sections served as positive controls. For immunofluorescence, antigen retrieval was performed in citrate buffer (pH 6.0, 95 °C, 20 min), followed by blocking in 5% goat serum containing 0.3% Triton X-100 for 1 h. Sections were incubated overnight at 4 °C with primary antibodies: Iba1 (1:500, Wako #019-19741), iNOS (1:200, Abcam #ab178945), and p-PI3K (1:300, CST #4228). Afterward, sections were incubated with Alexa Fluor-conjugated secondary antibodies (1:1000, Invitrogen) for 2 h. Negative controls omitted primary antibodies. Sections were mounted with Fluoromount-G containing DAPI.

Images were captured from five peri-infarct fields per section (×400 magnification) using a Zeiss Axio Imager M2 microscope by investigators blinded to treatment groups. ImageJ software quantified neuronal survival ($Nissl^+$ cells/mm^2), apoptosis (percentage of TUNEL-positive nuclei relative to DAPI), and fluorescence intensity (integrated density after background subtraction).

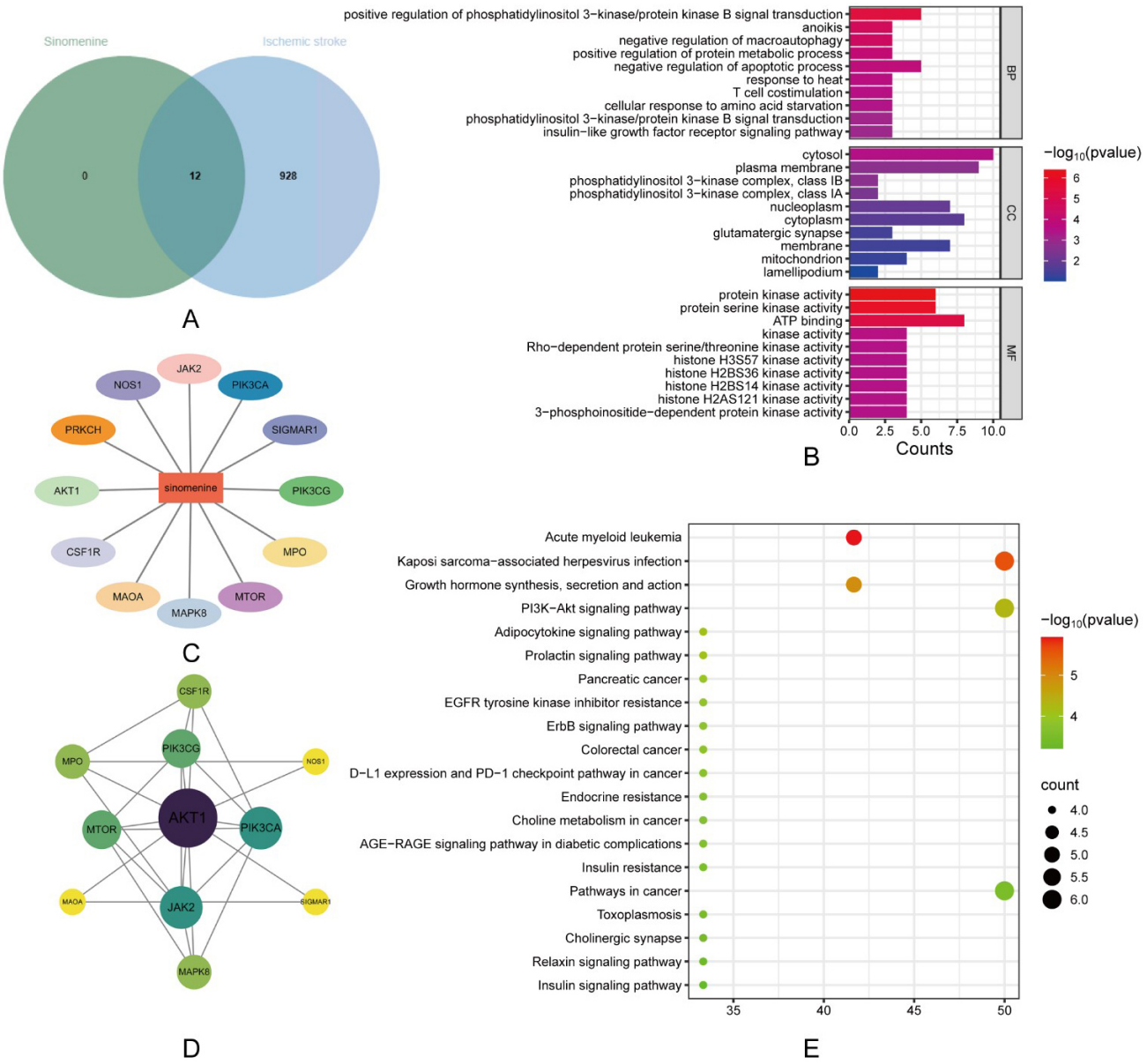

Fig. 1. Network pharmacology analysis of Sino against ischemic stroke. (A) Venn diagram illustrating overlap between Sino targets and ischemic stroke–related targets. (B) GO enrichment analysis. (C) Sino–target component interaction network. (D) PPI network of the 12 shared targets; node size corresponds to degree centrality, and edge thickness reflects interaction confidence scores. (E) KEGG pathway enrichment analysis. GO, Gene Ontology; PPl, protein-proteininteraction; KEGG, Kyoto Encyclopedia of Genes and Genomes.

2.8 Western Blot

Ischemic penumbra tissues were lysed in RIPA buffer containing protease and phosphatase inhibitors and centrifuged at 12,000 ×g for 15 min at 4 °C. Protein concentrations were determined using the BCA assay. Equal amounts of protein (30 µg per sample) were separated by 10% SDS-PAGE and transferred onto PVDF membranes (0.45 µm). Membranes were blocked with 5% non-fat milk in TBST for 1 h at room temperature and incubated overnight at 4 °C with primary antibodies against PI3K, p-PI3K (Tyr458), Akt, p-Akt (Ser473), Bax, Bcl-2, cleaved caspase-3 (Asp175), and β-actin (all diluted 1:1000). After washing, HRP-conjugated secondary antibodies (1:5000) were applied for 1 h at room temperature. Immunoreactive bands were visualized using enhanced chemiluminescence and captured on a ChemiDoc imaging system. Densitometric analysis was performed with ImageJ, normalizing target protein signals to β-actin loading controls. Results were expressed as fold changes relative to the sham group.

2.9 Enzyme-Linked Immunosorbent Assay (ELISA)

Pro-inflammatory cytokine levels in ischemic brain tissues were measured by ELISA. Ischemic hemispheres were homogenized in ice-cold phosphate-buffered saline

containing protease inhibitors and centrifuged at 10,000 ×g for 15 min at 4 °C. Clear supernatants were collected, and total protein concentrations were determined by BCA assay for normalization. Commercial ELISA kits were used to measure IL-1β, IL-6, and TNF-α following the manufacturer's protocols. Standards and samples were assayed in duplicate on pre-coated 96-well plates. After sequential incubation with biotinylated detection antibodies and HRP-conjugated streptavidin, chromogenic TMB substrate was added. Reactions were terminated with 2N sulfuric acid, and absorbance was read at 450 nm using a microplate spectrophotometer. Cytokine concentrations (pg/mL) were interpolated from standard curves, maintaining intra-assay coefficients of variation below 10%.

2.10 Statistical Analysis

Data were analyzed using SPSS software (version 26.0). Comparisons among multiple groups were conducted by one-way ANOVA followed by Tukey's post-hoc test. Two-way ANOVA was employed for longitudinal assessments of neurological function. Intergroup comparisons were performed using Student's *t*-test. In this study, n represents the number of biological replicates (independent animals) unless otherwise specified. All biochemical and histological assays were performed with technical triplicates (repeated measurements of the same sample) to ensure reproducibility. Results are presented as mean ± SD, and a p-value < 0.05 was considered statistically significant. All analyses were carried out by an investigator blinded to group assignments.

3. Results

3.1 Network Pharmacology Analysis of Sino Against Ischemic Stroke

3.1.1 Target Identification and Overlap Analysis

Twelve potential targets of Sino were identified through an integrated search of the TCMSP, SwissTargetPrediction, and PharmMapper databases. Concurrently, 940 ischemic stroke-related targets were retrieved from the GeneCards, OMIM, and DrugBank databases. Venn diagram analysis demonstrated that all 12 predicted Sino targets overlapped with those associated with ischemic stroke (Fig. 1A). This complete overlap suggests that the predicted target profile of Sino is functionally relevant to the pathological mechanisms underlying ischemic stroke.

3.1.2 Construction of the Component–Target Network

A component-target interaction network based on the 12 overlapping targets was constructed using Cytoscape (Fig. 1C). The resulting network displayed a characteristic "single compound–multiple targets" topology, comprising a single compound node (Sino) connected to 12 target nodes, namely Akt1, JAK2, PIK3CA, MAPK8, MTOR, PIK3CG, PRKCH, CSF1R, NOS1, MPO, MAOA, and SIGMAR1. This network architecture suggests that Sino may exert therapeutic effects on ischemic stroke by simultaneously modulating multiple molecular targets, consistent with the polypharmacological nature of natural compounds.

3.1.3 PPI Network Analysis

To further investigate interactions among the overlapping targets, a PPI network was constructed using the STRING database (Fig. 1D). This network revealed substantial interconnectivity among the 12 identified targets. Akt1, JAK2, PIK3CA, MAPK8, and MTOR showed relatively central positions and higher connectivity, indicating their roles as potential key regulatory nodes in the Sino pharmacological network against ischemic stroke. Notably, Akt1 was identified as the most prominent hub, suggesting its critical role in mediating the biological effects of Sino.

3.1.4 GO Functional Enrichment Analysis

GO enrichment analysis was conducted to characterize the biological functions associated with the overlapping targets (Fig. 1B). In the Biological Process (BP) category, significantly enriched terms included positive regulation of phosphatidylinositol 3-kinase/protein kinase B signaling, anoikis, negative regulation of macroautophagy, negative regulation of apoptosis, and T cell costimulation. In the Cellular Component (CC) category, targets were predominantly enriched in the cytosol, plasma membrane, class IA and class IB phosphatidylinositol 3-kinase complexes, cytoplasm, mitochondrion, and glutamatergic synapse. Major enriched terms in the Molecular Function (MF) category included ATP binding, protein kinase activity, protein serine/threonine kinase activity, and 3-phosphoinositide-dependent protein kinase activity. Collectively, these findings suggest that Sino's therapeutic effects may involve coordinated modulation of cell survival, inflammatory signaling, and kinase-related functions.

3.1.5 KEGG Pathway Enrichment Analysis

KEGG pathway enrichment analysis indicated that the 12 overlapping targets were significantly enriched in multiple signaling pathways (Fig. 1E). The primary enriched pathways included the PI3K/Akt signaling pathway, ErbB signaling pathway, PD-L1 expression and PD-1 checkpoint pathway in cancer, AGE-RAGE signaling pathway in diabetic complications, insulin resistance, and several cancer-related pathways. Notably, the PI3K/Akt pathway exhibited relatively high enrichment significance and a substantial target count, suggesting that it may constitute a core signaling mechanism underlying Sino's protective effects against ischemic stroke. These findings, coupled with Akt1's central position in the PPI network, support the hypothesis that the PI3K/Akt pathway is a critical mediator of Sino's pharmacological actions.

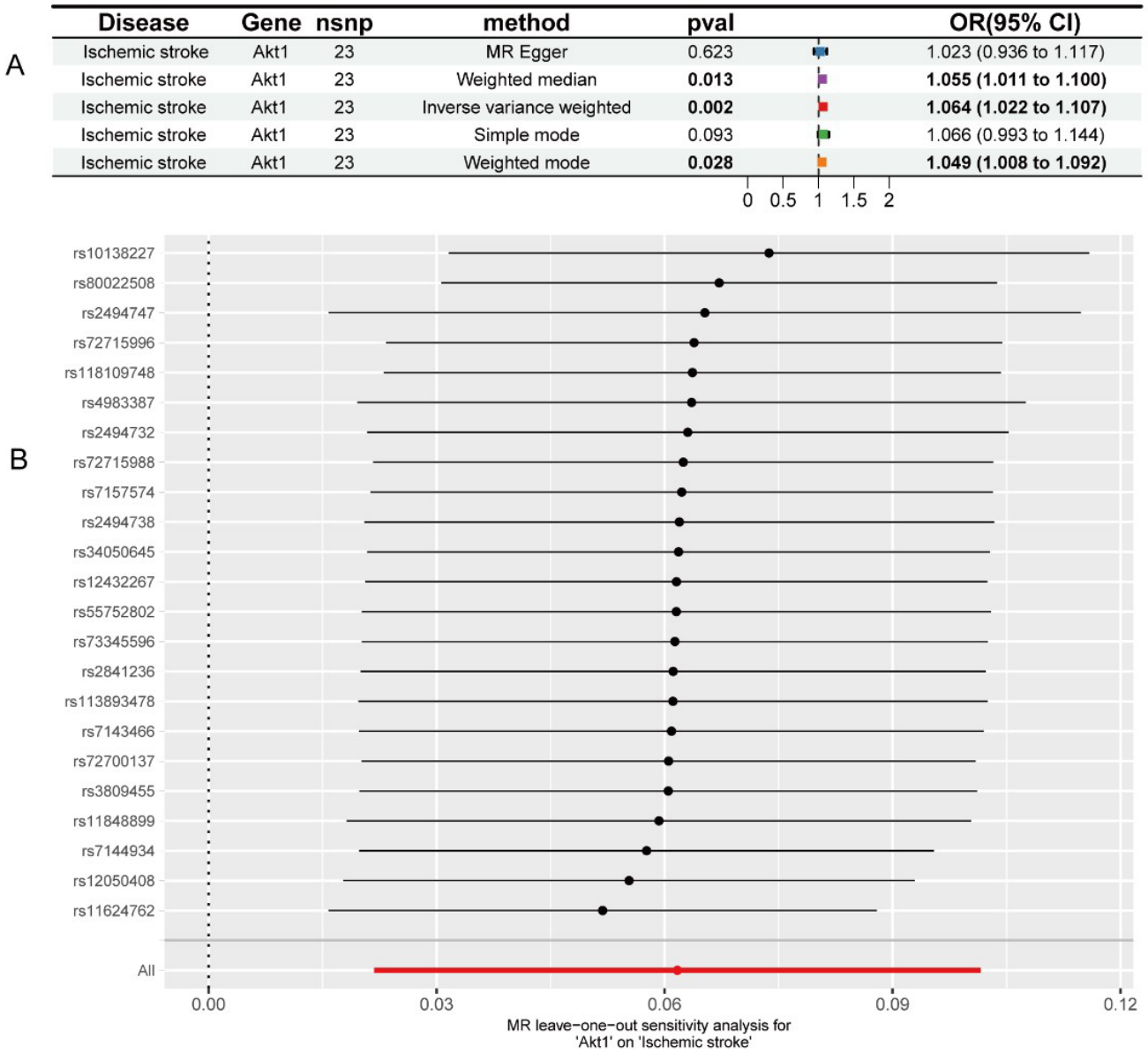

Fig. 2. Two-sample MR analysis of candidate targets for ischemic stroke. (A) Forest plot illustrating MR estimates for Akt1 obtained using various methods. cis-eQTLs for Akt1 (eQTLGen consortium) were instrumental variables, and ischemic stroke GWAS data (ebi-a-GCST90018864) were the outcomes. Methods include inverse variance weighted (IVW), weighted median, weighted mode, MR-Egger, and simple mode. Odds ratios (ORs) and 95% confidence intervals (CIs) are shown. (B) Sensitivity analyses for Akt1 include MR-Egger intercept testing for horizontal pleiotropy, Cochran's Q test for heterogeneity, and leave-one-out analysis assessing individual SNP influence on the IVW estimate. MR, Mendelian randomization; GWAS, Genome-wide association study; SNP, single nucleotide polymorphism.

3.2 MR Analysis

We conducted a two-sample MR analysis for each of the 12 candidate targets identified from NP. cis-eQTL data from the eQTLGen consortium served as instruments, with ischemic stroke GWAS data (ebi-a-GCST90018864) as the outcome. All selected instruments fulfilled criteria for genome-wide significance, independence, and exhibited F-statistics >10.

Among the 12 targets, only Akt1 demonstrated a nominal genetic association with ischemic stroke, highlighting its potential relevance. Employing 23 SNPs as instrumental variables (IVs) for Akt1, the inverse variance weighted (IVW) method yielded an OR of 1.064 (95% CI: 1.022–1.107, $p = 0.002$). The weighted median (OR = 1.055, $p = 0.013$) and weighted mode (OR = 1.049, $p = 0.028$) methods produced consistent findings, whereas MR-Egger and simple mode methods showed no significant associations

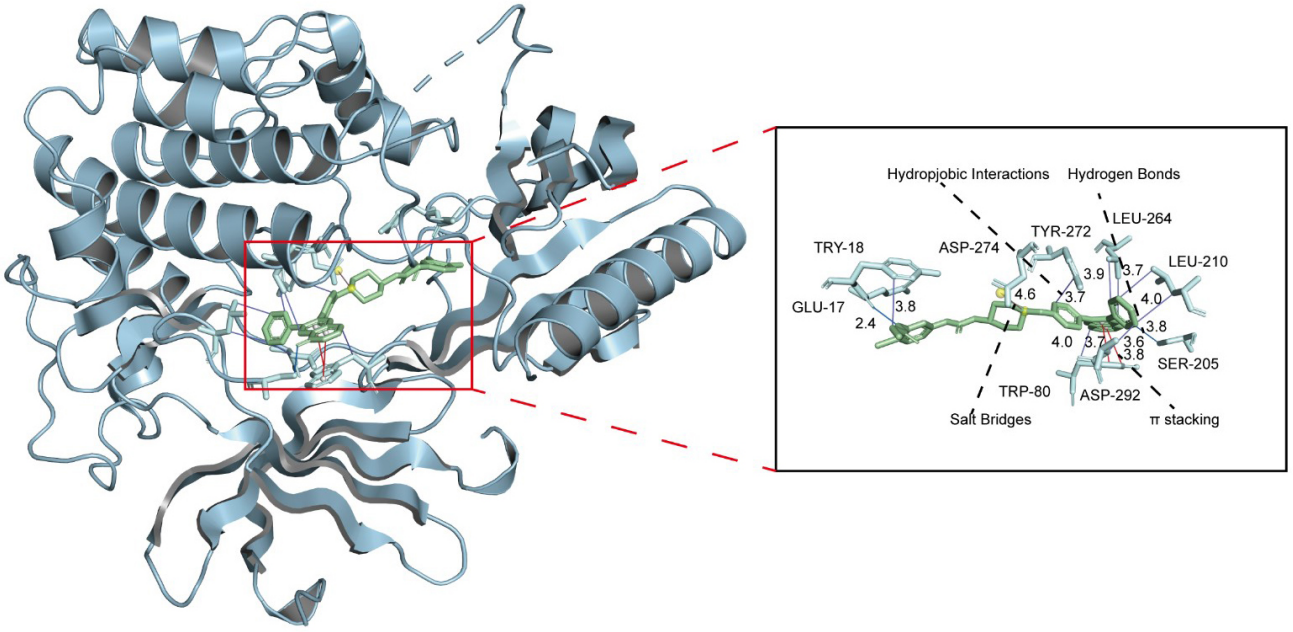

Fig. 3. Molecular docking conformation and interaction pattern of Sino with Akt1. The left panel shows a three-dimensional docking conformation of Sino (green) within the active pocket of Akt1 (PDB ID: 6HHG); the right panel presents a two-dimensional ligand-receptor interaction map. Interaction types are color-coded as follows: salt bridge, magenta-light pink; hydrogen bonds, marine blue; hydrophobic interactions, slate blue; π interactions, red.

(Fig. 2A). It is important to emphasize that this association reflects lifetime genetic exposure rather than acute pharmacological effects. The remaining 11 targets exhibited no significant causal effects in either IVW or alternative MR analyses ($p > 0.05$).

Sensitivity analyses for Akt1 confirmed the statistical robustness of this genetic association. Given MR's inherent limitations in capturing pharmacological dynamics, these results should be interpreted as hypothesis-generating, prioritizing Akt1 for further experimental investigation rather than providing direct mechanistic validation (Fig. 2B).

3.3 Molecular Docking Validation With Akt1

To structurally validate the interaction between Sino and the core target Akt1, molecular docking was performed using AutoDock Vina. Results demonstrated stable binding of Sino to the active pocket of Akt1, with a minimum binding energy of –5.97 kcal/mol, indicative of a favorable affinity. Detailed interaction analysis revealed hydrogen bonds, π-π stacking, salt bridge formation, and hydrophobic interactions between Sino and Akt1 (Fig. 3). Specifically, hydrogen bonding involved key residues TRP80, GLU17, and SER205; π-π stacking primarily involved TRP80; salt bridges involved ASP274; and hydrophobic interactions involved residues TYR18, LEU210, LEU264, TYR272, and ASP292. These results indicate that Sino achieves a stable binding conformation with Akt1, providing structural support for its regulation of the PI3K/Akt signaling pathway and associated neuroprotective effects.

3.4 Neuroprotective Effects of Sino in a Rat Model of Cerebral Ischemia/Reperfusion

3.4.1 Neurological Function Assessment

To assess Sino's effects on neurological deficits following AIS, neurological function was evaluated using the Zea-Longa score, Bederson score, and modified Garcia score (Fig. 4A–C). Compared with the Sham group, the MCAO/R group exhibited significant neurological impairments, characterized by significantly elevated Zea-Longa and Bederson scores and a notably reduced modified Garcia score ($p < 0.0001$). Sino treatment significantly mitigated neurological deficits, decreasing the Zea-Longa score from 3.167 ± 0.3892 to 1.167 ± 0.3892 ($p < 0.0001$), reducing the Bederson score from 1.545 ± 0.5222 to 0.7917 ± 0.3343 ($p = 0.0003$), and increasing the modified Garcia score from 12.75 ± 0.8660 to 15.17 ± 1.267 ($p < 0.0001$). However, co-treatment with LY significantly weakened Sino's neuroprotective effect, as evidenced by an increased Zea-Longa score to 2.000 ± 0.6030 (vs. Sino, $p < 0.0001$), increased Bederson score to 1.333 ± 0.4924 (vs. Sino, $p = 0.0104$), and decreased modified Garcia score to 11.25 ± 0.7538 (vs. Sino, $p < 0.0001$). These findings suggest Sino markedly alleviates neurological deficits following AIS, whereas PI3K inhibition partially reverses these protective effects, implicating involvement of the PI3K/Akt signaling pathway in Sino-mediated neuroprotection.

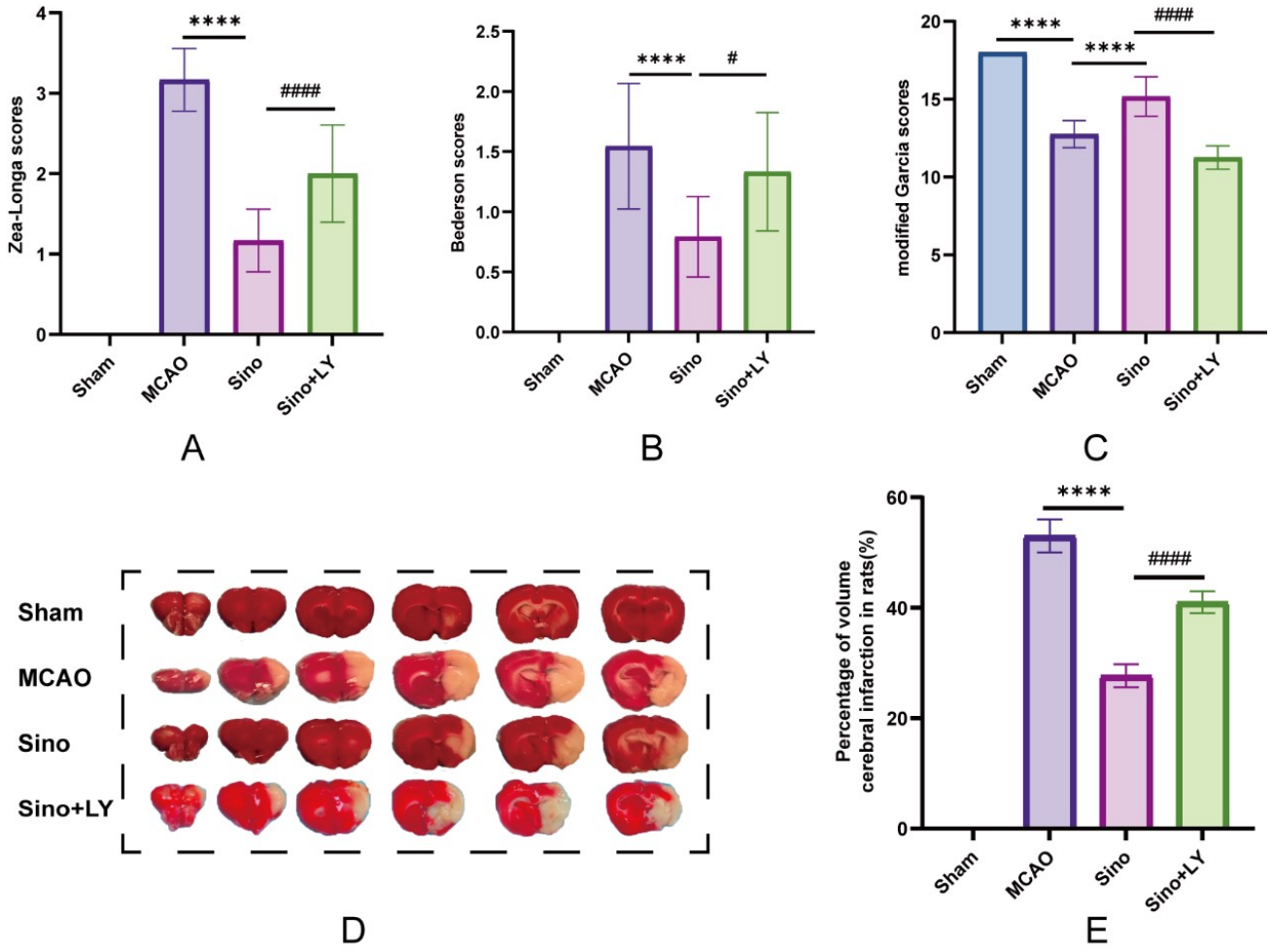

Fig. 4. Effects of Sino on neurological deficits and cerebral infarct volume in MCAO/R rats. (A) Zea-Longa score (n = 12). (B) Bederson score. (C) Modified Garcia score. (D) Representative TTC-stained coronal brain sections (n = 3). (E) Quantitative analysis of infarct volume. Data are expressed as mean ± SD. **** $p < 0.0001$ vs. Sham group; $^{\#}$ $p < 0.05$, $^{\#\#\#\#}$ $p < 0.0001$ vs. Sino group.

3.4.2 Infarct Volume Measurement and TTC Staining

TTC staining revealed no visible infarction in the Sham group, with an infarct volume percentage of 0.000 ± 0.000. Conversely, the MCAO/R group exhibited a substantial increase in infarct volume (53.00 ± 3.000), significantly different from the Sham group ($p < 0.0001$), confirming the presence of cerebral infarction post-AIS. MCAO/RSino treatment significantly reduced infarct volume to 27.67 ± 2.082 ($p < 0.0001$) compared to the MCAO/R group, demonstrating a pronounced protective effect against ischemic damage. However, in the Sino + LY group, infarct volume increased to 41.00 ± 2.000 ($p = 0.0002$ vs. Sino), indicating that LY treatment partially reversed Sino's neuroprotection (Fig. 4D,E). These results suggest that Sino significantly attenuates cerebral infarction induced by ischemia/reperfusion injury, potentially through modulation of the PI3K/Akt signaling pathway.

3.4.3 Histopathological Observations

TUNEL and Nissl staining further confirmed the neuroprotective effects of Sino against ischemia/reperfusion injury (Fig. 5). TUNEL staining demonstrated a marked increase in apoptotic cells in the MCAO/R group, with the apoptotic index significantly higher than that in the Sham group (51.13 ± 1.464 vs. 6.100 ± 0.7000, $p < 0.0001$). Sino treatment significantly reduced the apoptotic index to 21.47 ± 0.8505 ($p < 0.0001$ vs. MCAO/R), whereas co-treatment with LY increased it to 31.73 ± 1.405 ($p < 0.0001$ vs. Sino), suggesting that PI3K inhibition partially reversed the anti-apoptotic effect of Sino. Nissl staining showed that the the density of Nissl-positive neurons (cells/mm²) in the MCAO/R group was significantly lower than that in the Sham group (44.33 ± 3.055 vs. 98.00 ± 3.606, $p < 0.0001$), indicating substantial neuronal damage following ischemia/reperfusion injury. Sino treatment significantly increased the density of Nissl-positive neurons (cells/mm²) to 75.00 ± 3.000 ($p < 0.0001$ vs. MCAO/R), whereas co-treatment with LY reduced it to 60.33 ± 2.517 ($p = 0.0017$

vs. Sino), indicating that LY partially attenuated the neuroprotective effect of Sino. These findings suggest that Sino significantly inhibited apoptosis and alleviated neuronal damage after ischemia/reperfusion injury, potentially through the PI3K/Akt signaling pathway.

3.4.4 Western Blot

Western blot analysis demonstrated that Sino markedly modulated PI3K/Akt signaling activation and the expression of apoptosis-related proteins (Fig. 6A–F). Compared with the Sham group, the p-PI3K/PI3K level in the MCAO/R group showed an increasing trend but did not reach statistical significance (0.7496 ± 0.08713 vs. 0.6387 ± 0.08246, $p = 0.5981$), whereas the p-Akt/Akt level was significantly reduced (0.3825 ± 0.02338 vs. 0.5787 ± 0.04226, $p < 0.0001$). Meanwhile, the expression of pro-apoptotic proteins Bax and cleaved caspase-3 increased significantly from 0.1460 ± 0.03507 and 0.4340 ± 0.05273 to 0.8240 ± 0.07021 and 1.000 ± 0.05916, respectively (both $p < 0.0001$), while the anti-apoptotic protein Bcl-2 decreased from 0.8920 ± 0.02775 to 0.5600 ± 0.05099 ($p < 0.0001$), indicating that ischemia/reperfusion injury suppressed Akt activation and disrupted the balance of apoptosis-related proteins. Compared with the MCAO/R group, the p-PI3K/PI3K and p-Akt/Akt levels in the Sino group increased significantly to 1.511 ± 0.2293 and 0.7770 ± 0.03517, respectively (both $p < 0.0001$). Concurrently, Bax and cleaved caspase-3 expression decreased significantly to 0.4200 ± 0.07416 and 0.5940 ± 0.06229 (both $p < 0.0001$), whereas Bcl-2 expression increased to 1.042 ± 0.07563 ($p < 0.0001$), indicating activation of the PI3K/Akt pathway and suppression of pro-apoptotic signaling. In the Sino + LY group, the p-PI3K/PI3K and p-Akt/Akt levels decreased to 0.7550 ± 0.1007 and 0.3717 ± 0.03496, respectively (both $p < 0.0001$ vs. Sino). Meanwhile, Bax and cleaved caspase-3 expression increased to 1.062 ± 0.1190 and 0.8480 ± 0.04087 (both $p < 0.0001$), whereas Bcl-2 decreased to 0.5420 ± 0.04438 ($p < 0.0001$), suggesting that LY attenuated the regulatory effects of Sino on PI3K/Akt signaling and apoptosis-related proteins. These results indicate that Sino may exert anti-apoptotic and neuroprotective effects by activating the PI3K/Akt pathway, upregulating Bcl-2, and downregulating Bax and cleaved caspase-3.

3.4.5 Immunofluorescence Analysis of Brain Tissue

Immunofluorescence staining demonstrated that Sino significantly regulated the expression of iNOS, p-PI3K, and Iba1 (Fig. 7). Compared with the Sham group, the MCAO/R group showed markedly increased iNOS expression (3.047 ± 0.1014 vs. 0.9927 ± 0.05637, $p < 0.0001$) and significantly reduced p-PI3K expression (0.6573 ± 0.02764 vs. 0.9927 ± 0.05637, $p < 0.0001$), indicating enhanced inflammatory responses and suppressed PI3K signaling following ischemia/reperfusion injury. In addition, Iba1-positive signals were substantially elevated in the MCAO/R group compared with the Sham group (30.14 ± 2.782 vs. 1.000 ± 0.6962, $p < 0.0001$), suggesting pronounced microglial activation. Compared with the MCAO/R group, the Sino group exhibited significantly reduced iNOS expression (1.347 ± 0.06508, $p < 0.0001$), increased p-PI3K expression (1.339 ± 0.05805, $p < 0.0001$), and decreased Iba1-positive signals (11.17 ± 1.390, $p < 0.0001$), indicating suppression of inflammatory responses, activation of the PI3K pathway, and attenuation of microglial activation. In contrast, the Sino + LY group showed increased iNOS expression (3.118 ± 0.05672, $p < 0.0001$ vs. Sino), decreased p-PI3K expression (0.6153 ± 0.02669, $p < 0.0001$), and elevated Iba1-positive signals (21.00 ± 2.001, $p < 0.0001$), indicating that LY diminished the regulatory effects of Sino on inflammation, microglial activation, and PI3K signaling. These findings suggest that Sino may exert anti-inflammatory and neuroprotective effects through activation of the PI3K pathway, inhibition of iNOS expression, and suppression of microglial activation.

3.4.6 Levels of Inflammatory Cytokines in Brain Tissue

ELISA results showed a significant increase in inflammatory response in brain tissue following ischemia/reperfusion injury (Fig. 8). Compared with the Sham group, the MCAO/R group had significantly elevated levels (pg/mL) of IL-1β (477.6 ± 20.37 vs. 212.6 ± 21.29), IL-6 (3201 ± 46.00 vs. 1010 ± 12.74), and TNF-α (58.39 ± 1.388 vs. 18.84 ± 0.9431) (all $p < 0.0001$), demonstrating substantial cytokine release triggered by ischemic insult. Sino treatment significantly reduced IL-1β, IL-6, and TNF-α levels to 272.4 ± 6.528, 2070 ± 70.83, and 38.59 ± 1.116, respectively (all $p < 0.0001$ vs. MCAO/R), indicating robust suppression of inflammatory response by Sino. However, co-treatment with LY reversed this effect, increasing cytokine levels back to 468.1 ± 5.910, 3398 ± 31.18, and 59.04 ± 0.8494, respectively (all $p < 0.0001$ vs. Sino). These results suggest that Sino effectively attenuated ischemia/reperfusion-induced inflammation, possibly through the PI3K/Akt signaling pathway.

4. Discussion

In this exploratory study, we established a convergent validation framework integrating NP, MR, molecular docking, and pharmacological rescue experiments to dissect the neuroprotective mechanisms of Sino in ischemic stroke. Rather than treating these approaches as sequential and independent, we positioned them as mutually reinforcing layers of evidence: NP provided a systems-level target landscape, MR facilitated population-scale genetic prioritization, docking yielded structural plausibility, and the LY-mediated rescue experiment supplied causal, pathway-specific functional evidence. This multi-dimensional integration represents a methodological advance over conventional single-strategy preclinical studies, which often suffer

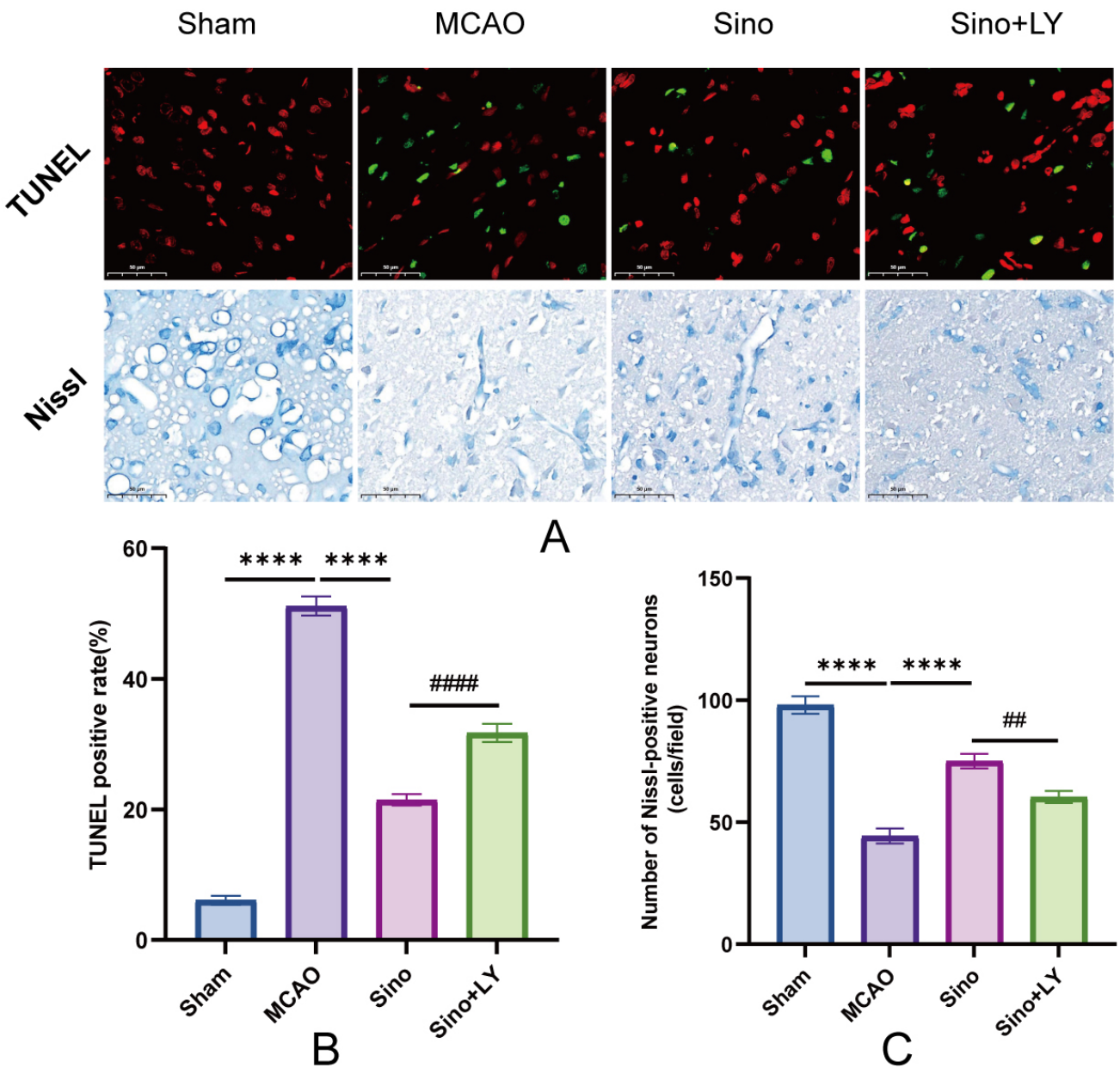

Fig. 5. Effects of Sino on neuronal apoptosis and neuronal injury in MCAO/R rats. (A) Representative TUNEL and Nissl staining images in the Sham, MCAO/R, Sino, and Sino + LY groups. Red fluorescence indicates DAPI-stained nuclei, whereas green fluorescence indicates TUNEL-positive apoptotic cells (×400). Scale bar, 50 µm. (B) Quantification of the TUNEL-positive rate. (C) Quantification of Nissl-positive neurons (cells/mm²). Data are expressed as mean ± SD. **** $p < 0.0001$ vs. Sham group; $^{\#\#}$ $p < 0.01$, $^{\#\#\#\#}$ $p < 0.0001$ vs. Sino group. n = 3.

either from computational overprediction lacking experimental support or *in vivo* observations without clear mechanistic grounding [20,21]. By enforcing convergence across computational, genetic, and pharmacological domains, we prioritized PI3K/Akt as a high-confidence hub and subsequently validated its functional relevance within a coherent biological context.

The convergence of NP, MR, and structural docking on Akt1 merits particular emphasis. NP analysis identified Akt1 as the topological hub within the Sino-stroke target interactome, while KEGG enrichment analyses consistently highlighted the PI3K/Akt pathway. Additionally, MR analysis provided supportive, albeit modest, genetic evidence linking cis-regulated Akt1 expression to ischemic stroke risk (IVW OR = 1.064, $p = 0.002$). This MR finding warrants cautious interpretation, reflecting lifelong, tissue-averaged genetic exposure rather than acute pharmacological modulation in post-ischemic brain conditions [22]. The apparent paradox, where genetically predicted higher Akt1 expression associates with increased stroke

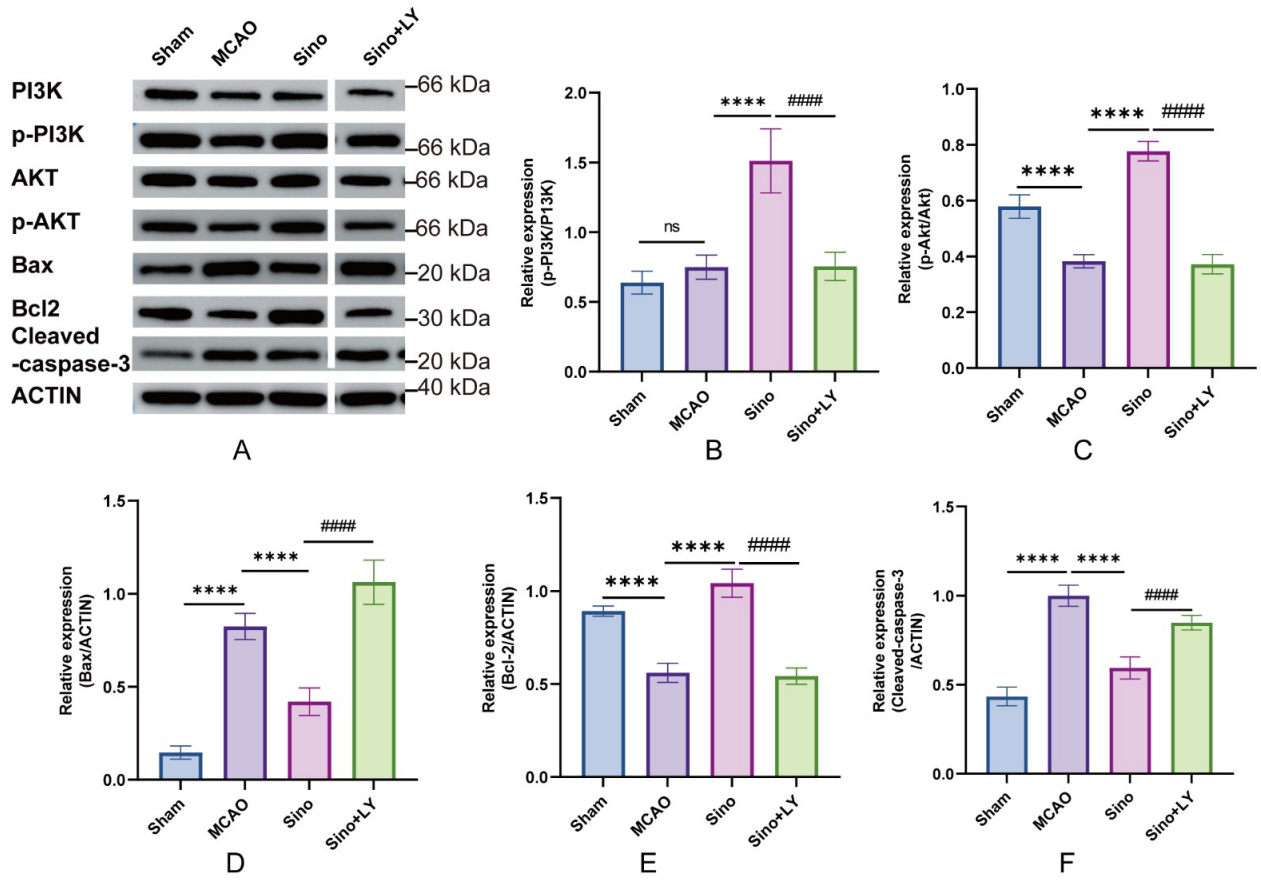

Fig. 6. Effects of Sino on PI3K/Akt signaling and apoptosis-related proteins in MCAO/R rats. (A) Representative Western blot images of PI3K, p-PI3K, Akt, p-Akt, Bax, Bcl-2, cleaved caspase-3, and ACTIN. (B) p-PI3K/PI3K ratio. (C) p-Akt/Akt ratio. (D) Bax/β-actin. (E) Bcl-2/β-actin. (F) Cleaved caspase-3/β-actin. Data are expressed as mean ± SD. ns, not significant; **** $p < 0.0001$ vs. Sham group; #### $p < 0.0001$ vs. Sino group. n = 5.

risk, while acute pharmacological activation appears protective, likely arises due to differences in cell-type specificity (endothelial, neuronal, or microglial), chronic compensatory feedback loops, or horizontal pleiotropy inherent in cis-eQTL instruments. Rather than viewing this discrepancy as contradictory, we consider it indicative of the context-dependent nature of pathway biology. Importantly, the MR finding fulfilled its role as a genetic prioritization filter, focusing experimental resources on Akt1 among the 12 candidate targets. Subsequent molecular docking analysis confirmed structural compatibility, revealing a binding energy of –5.97 kcal/mol, stabilized by hydrogen bonding, π–π stacking, and hydrophobic interactions within the Sino-Akt1 complex. Therefore, computational prediction, genetic prioritization, structural validation, and functional rescue collectively provide a robust, multi-layered rationale supporting the central mechanistic role of PI3K/Akt.

From a pathophysiological perspective, cerebral ischemia/reperfusion injury initiates an interconnected amplification cascade encompassing excitotoxicity, oxidative stress, neuroinflammation, blood–brain barrier disruption, and regulated cell death. These processes are not isolated parallel events but constitute a network-like pathological system in which mitochondrial dysfunction and inflammatory signaling reciprocally amplify each other. The PI3K/Akt pathway occupies a central regulatory node within this network, simultaneously governing neuronal survival via BCL-2 family modulation and inflammatory tone via NF-κB-dependent transcriptional control. Our findings demonstrate that ischemia/reperfusion suppressed Akt phosphorylation without altering total protein abundance, indicating a state of functional inactivation rather than transcriptional loss [21]. Sino restored p-PI3K and p-Akt levels, concurrently shifting the apoptotic balance toward survival (Bcl-2 upregulation, Bax and cleaved caspase-3 downregulation) and suppressing microglial activation (Iba1 and iNOS reduction) alongside pro-inflammatory cytokine attenuation (IL-1β, IL-6, TNF-α) [21,23]. These coordinated molecular changes suggest that Sino does not merely modulate individual downstream events but engages a higher-order pathway-level regulatory mechanism, reinstating homeostatic control over the apoptosis–inflammation axis [20,21].

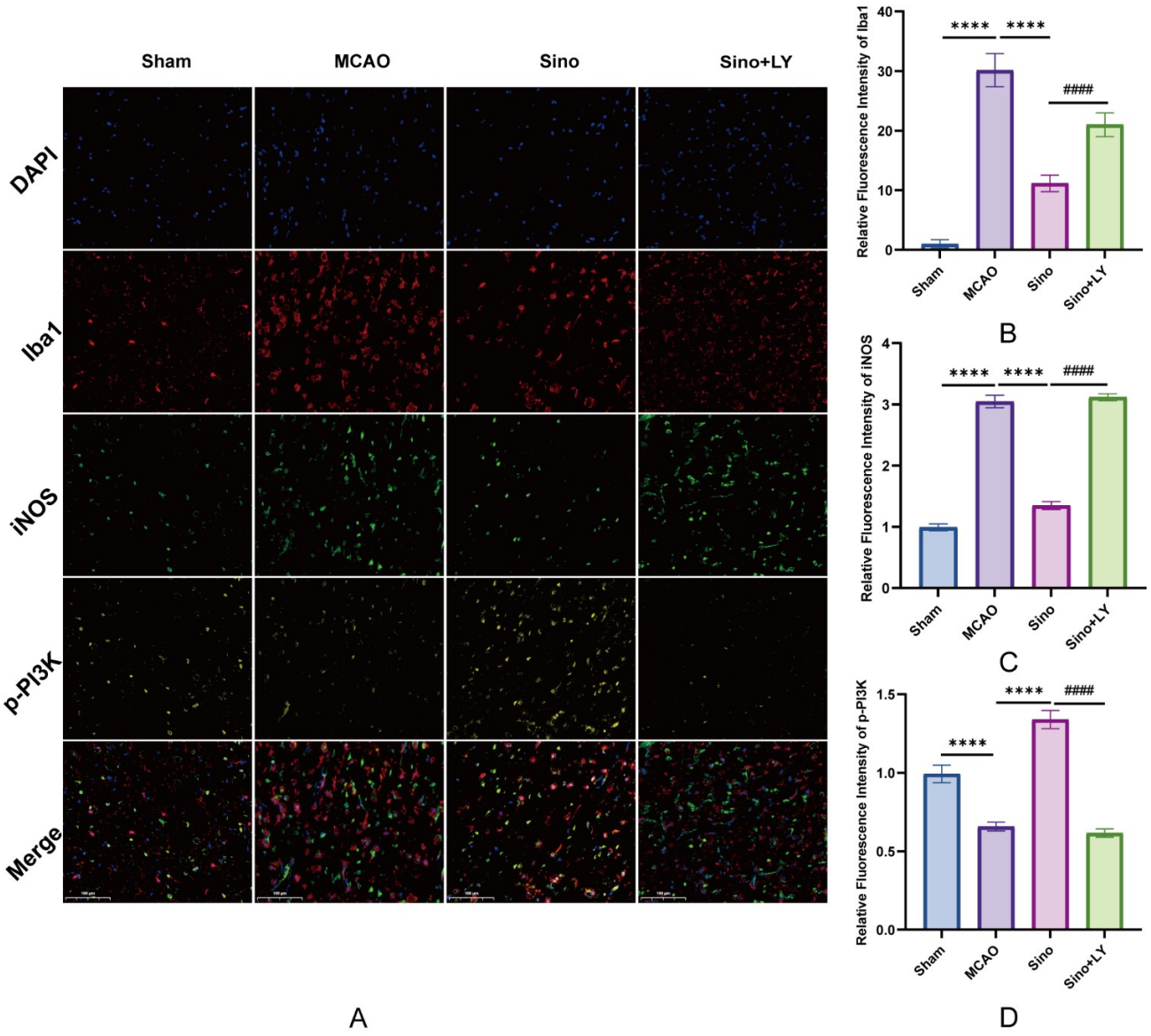

Fig. 7. Effects of Sino on microglial activation, inflammatory marker expression, and PI3K signaling in MCAO/R rats. (A) Representative immunofluorescence staining images for Iba1, iNOS, and p-PI3K in each group(×200). (B) Quantitative analysis of Iba1 fluorescence intensity. (C) Quantitative analysis of iNOS fluorecence intensity. (D) Quantitative analysis of p-PI3K fluorescence intensity. Scale bar, 100 μm. Data are expressed as mean ± SD. **** $p < 0.0001$ vs. Sham group; #### $p < 0.0001$ vs. Sino group. n = 3.

Neuroinflammation represents another critical driver of secondary brain injury following ischemic stroke and is closely associated with BBB dysfunction, innate immune activation, and thromboinflammatory interactions [20,24]. Clinical and experimental studies have shown that BBB disruption facilitates infiltration of peripheral immune cells, while resident microglia rapidly respond to ischemic injury. Persistent activation of pro-inflammatory pathways leads to excessive release of cytokines, reactive oxygen species, and nitric oxide, exacerbating neuronal injury and amplifying apoptosis [24]. In the present study, MCAO/R induced a robust pro-inflammatory microglial response, characterized by increased Iba1 expression and an M1-like phenotype with elevated levels of iNOS, IL-1β, IL-6, and TNF-α. These markers are well-established indicators of detrimental microglial activation following cerebral ischemia [25]. Sino substantially attenuated these inflammatory responses, indicating its modulatory effects on the inflammatory microenvironment after stroke. Notably, restoration of PI3K/Akt phosphorylation coincided with suppression of inflammatory markers, supporting the hypothesis that Sino may partially exert anti-inflammatory effects through PI3K/Akt-mediated negative regulation of inflammation. Previous reviews have highlighted that PI3K/Akt signaling can restrain NF-κB activation and facilitate a shift away from harmful M1-like microglial phenotypes under certain conditions [20,25]. Although the present study does not establish causality regarding whether PI3K/Akt activation

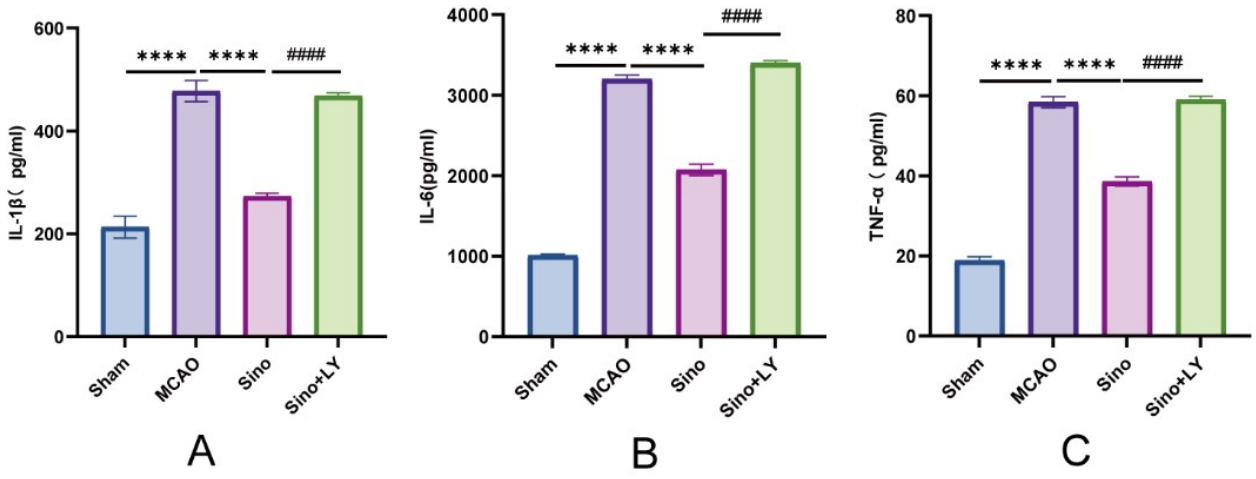

Fig. 8. Effects of Sino on inflammatory cytokine levels in the ischemic hemisphere. (A) IL-1β levels. (B) IL-6 levels. (C) TNF-α levels. Data are expressed as mean ± SD. **** $p < 0.0001$ vs. Sham group; #### $p < 0.0001$ vs. Sino group. n = 3.

drives inflammation suppression or vice versa, the coherent improvements observed across functional, histological, and molecular domains support the biological plausibility of coordinated pathway-level regulation.

The pharmacological inhibition experiment with LY provides critical causal evidence supporting PI3K/Akt as a necessary mediator of Sino-induced neuroprotection. LY is a highly specific PI3K inhibitor that competes with ATP for binding to the p110 catalytic subunit, thereby blocking downstream Akt phosphorylation independently of upstream receptor activation [26]. In our study, co-administration of LY not only abolished Sino-induced PI3K/Akt phosphorylation but also quantitatively reversed its protective effects, neurological recovery, infarct reduction, neuronal survival, and anti-inflammatory responses, toward MCAO/R baseline levels. This "rescue-to-baseline" pattern satisfies the classical criteria for pharmacological epistasis: if inhibition of a specific signaling node abolishes the drug effect, then the effect is mechanistically dependent on that node [27]. Therefore, LY treatment converts correlational observations into functional causality, establishing PI3K/Akt activation as a necessary component of Sino-mediated neuroprotection rather than a mere associative biomarker. Notably, LY did not fully restore all parameters to MCAO/R severity, suggesting that Sino may retain partial PI3K/Akt-independent effects or that compensatory pathways partially buffer against acute PI3K inhibition [14]. This incomplete reversal, rather than weakening the conclusion, supports the interpretation that Sino acts as a multi-target agent, with PI3K/Akt serving as a dominant but not exclusive effector axis [14,15].

Despite decades of preclinical promise, nearly all single-target neuroprotective agents have failed in human stroke trials, largely due to the inability of monotherapies to disrupt the multi-pathway, self-amplifying cascades of ischemic brain injury [28,29]. Sino, as a plant-derived alkaloid, exhibits inherent polypharmacological properties [14,15]. Our data indicate that Sino concurrently suppresses neuronal apoptosis, microglial M1-like polarization, and pro-inflammatory cytokine release through PI3K/Akt-dependent and potentially PI3K/Akt-independent mechanisms. This multi-modal activity is consistent with the emerging paradigm that effective stroke neuroprotection requires coordinated modulation of multiple injury pathways rather than precise targeting of a single molecule [29]. Compared with synthetic kinase inhibitors, which often face safety limitations (e.g., on-target toxicity and narrow therapeutic windows), natural compounds such as Sino may offer a more favorable risk–benefit profile due to moderate binding affinities across multiple targets and established clinical use in rheumatic diseases [14]. Furthermore, the post-stroke therapeutic window evaluated in this study (initiation within 6 hours and continuation for 3 days) reflects a clinically relevant scenario for patients presenting after reperfusion therapy [2,20]. We propose that Sino's ability to simultaneously attenuate neuroinflammation and preserve neuronal viability through pathway-level PI3K/Akt modulation positions it as a promising adjunctive neuroprotective candidate, particularly in combination with reperfusion strategies to mitigate secondary injury during the hyperacute and early subacute phases [29].

5. Limitations

Several limitations should be acknowledged. First, the NP analysis depended on publicly available databases, which might contain incomplete or biased target information. Second, although MR provided genetic evidence supporting Akt1 prioritization, this method reflects lifelong genetic exposure and cannot directly elucidate acute pharmacological mechanisms of Sino action. Third, *in vivo* validation was conducted in a single rat MCAO/R model with a relatively short observation period, potentially insufficient

for capturing the long-term neuroprotective effects of Sino. Fourth, while LY was utilized to validate PI3K/Akt pathway involvement, further mechanistic studies are necessary to clarify upstream regulators and downstream signaling networks. Finally, the translation of these findings to clinical ischemic stroke requires additional validation in diverse experimental models and, ultimately, human studies.

6. Conclusion

In summary, this study establishes a multi-dimensional validation framework integrating network pharmacology, Mendelian randomization, molecular docking, and pharmacological rescue experiments to demonstrate that Sino confers protection against experimental ischemic stroke via PI3K/Akt-dependent coordination of anti-apoptotic and anti-inflammatory responses. LY-mediated pathway inhibition functionally confirms PI3K/Akt as a necessary causal mediator, while its incomplete reversal highlights Sino's multi-target therapeutic profile. In the context of repeated failures of single-target neuroprotective strategies in clinical stroke trials, Sino's capacity to modulate convergent signaling hubs supports its potential as a promising adjunctive agent in the reperfusion era. Further studies should focus on elucidating upstream regulatory triggers, downstream pathway specificity, and optimizing brain-targeted delivery strategies to facilitate clinical translation.

Abbreviations

PI3K/Akt, The phosphatidylinositol 3-kinase/protein kinase B; MR, Mendelian randomization; MCAO, Middle cerebral artery occlusion; NF-κB, the nuclear factor-κB; GO, Gene Ontology; KEGG, Kyoto Encyclopedia of Genes and Genomes; PPI, protein-protein interaction; DMSO, dissolved in dimethyl sulfoxide; ELISA, Enzyme-linked immunosorbent assay; HE, Hematoxylin and Eosin staining; BBB, Blood-brain barrier.

Availability of Data and Materials

The datasets used and analyzed in this study are accessible from the corresponding author, Miao Qu, provided the request is reasonable.

Author Contributions

XQ designed and performed the experiments, analyzed the data, and wrote the manuscript. YD conducted network pharmacology and MR analysis. XL and WZ assisted with animal experiments and data collection. MQ and LW designed the study and supervised the project; MQ serves as the corresponding author. All authors edited, read, and approved the final manuscript, and agreed to be accountable for all aspects of the work.

Ethics Approval and Consent to Participate

All animal studies were approved by the Institutional Animal Care and Use Committee of Capital Medical University (Approval No. AEEI-2024-129). Animals were maintained and experiments were conducted in compliance with: the Guide for the Care and Use of Laboratory Animals (National Research Council, USA, 8th edition, 2011);the ARRIVE Guidelines 2.0 (Percie du Sert et al., 2020) for transparent reporting of animal research;the 3Rs principle as outlined by Russell and Burch (1959).

Acknowledgment

We gratefully acknowledge the assistance and instruction from the staff at the Animal Facility of Capital Medical University and our laboratory colleagues.

Funding

This research was funded by the National Natural Science Foundation of China (Grant No. 82274444).

Conflicts of Interest

The authors declare no conflicts of interest.

Declaration of AI and AI-Assisted Technologies in the Writing Process

During the preparation of this work the authors used ChatGpt-3.5 in order to check spell and grammar. After using this tool, the authors reviewed and edited the content as needed and takes full responsibility for the content of the publication.

Supplementary Material

Supplementary material associated with this article can be found, in the online version, at https://doi.org/10.31083/FBL50007.

References

[1] Qin F, Zhao Y, Shang W, Zhao ZM, Qian X, Zhang BB, et al. Sinomenine relieves oxygen and glucose deprivation-induced microglial activation via inhibition of the SP1/miRNA-183-5p/IκB-α signaling pathway. Cellular and Molecular Biology (Noisy-le-Grand, France). 2018; 64: 140–147. https://doi.org/10.14715/cmb/2018.64.10.23

[2] Campbell B, Khatri P. Stroke. Lancet (London, England). 2020; 396: 129–142. https://doi.org/10.1016/S0140-6736(20)31179-X

[3] Iadecola C, Anrather J. The immunology of stroke: from mechanisms to translation. Nature Medicine. 2011; 17: 796–808. https://doi.org/10.1038/nm.2399

[4] Zhu Y, Zhang J, Deng Q, Chen X. Mitophagy-associated programmed neuronal death and neuroinflammation. Frontiers in immunology. 2024; 15: 1460286. https://doi.org/10.3389/fimmu.2024.1460286

[5] Fang Y, Gao S, Wang X, Cao Y, Lu J, Chen S, et al. Programmed Cell Deaths and Potential Crosstalk With Blood-Brain Barrier Dysfunction After Hemorrhagic Stroke. Frontiers in Cel-

lular Neuroscience. 2020; 14: 68. https://doi.org/10.3389/fncel.2020.00068
[6] Song G, Ouyang G, Bao S. The activation of Akt/PKB signaling pathway and cell survival. Journal of Cellular and Molecular Medicine. 2005; 9: 59–71. https://doi.org/10.1111/j.1582-4934.2005.tb00337.x
[7] Liu M, Huang X, Tian Y, Yan X, Wang F, Chen J, et al. Phosphorylated GSK-3β protects stress-induced apoptosis of myoblasts via the PI3K/Akt signaling pathway. Molecular Medicine Reports. 2020; 22: 317–327. https://doi.org/10.3892/mmr.2020.11105
[8] Xu H, Qin W, Hu X, Mu S, Zhu J, Lu W, et al. Lentivirus-mediated overexpression of OTULIN ameliorates microglia activation and neuroinflammation by depressing the activation of the NF-κB signaling pathway in cerebral ischemia/reperfusion rats. Journal of Neuroinflammation. 2018; 15: 83. https://doi.org/10.1186/s12974-018-1117-5
[9] Guo N, Wang X, Xu M, Bai J, Yu H, Le Zhang. PI3K/AKT signaling pathway: Molecular mechanisms and therapeutic potential in depression. Pharmacological Research. 2024; 206: 107300. https://doi.org/10.1016/j.phrs.2024.107300
[10] Xu JL, Che HJ, Yang ZZ, Yang M. Research advances in the neuroprotective effect of natural drugs in ischemic stroke. Journal of QingDao University(Medical Sciences). 2025; 61: 312–316. https://doi.org/10.11712/jms.2096-5532.2025.61.050 (In Chinese)
[11] Yan M, Ni F, Xie X, Zhang C, Zhu J. The Role of Formononetin in Cerebral Ischemia-Reperfusion Injury: A New Mediator of c-Fos/IL-10/STAT3 Signaling Pathway. Frontiers in Bioscience (Landmark Edition). 2025; 30: 26274. https://doi.org/10.31083/fbl26274
[12] Chen J, Zhu L, Chen Y, Liu Y, Chen W, Liu X, et al. Targeted neural stem cell-derived extracellular vesicles loaded with Sinomenine alleviate diabetic peripheral neuropathy via WNT5a/TRPV1 pathway modulation. Journal of Nanobiotechnology. 2025; 23: 588. https://doi.org/10.1186/s12951-025-03678-3
[13] Wang Q, Li XK. Immunosuppressive and anti-inflammatory activities of sinomenine. International Immunopharmacology. 2011; 11: 373–376. https://doi.org/10.1016/j.intimp.2010.11.018
[14] Hong H, Lu X, Lu Q, Huang C, Cui Z. Potential therapeutic effects and pharmacological evidence of sinomenine in central nervous system disorders. Frontiers in Pharmacology. 2022; 13: 1015035. https://doi.org/10.3389/fphar.2022.1015035
[15] Qiu J, Yan Z, Tao K, Li Y, Li Y, Li J, et al. Sinomenine activates astrocytic dopamine D2 receptors and alleviates neuroinflammatory injury via the CRYAB/STAT3 pathway after ischemic stroke in mice. Journal of Neuroinflammation. 2016; 13: 263. https://doi.org/10.1186/s12974-016-0739-8
[16] Biose IJ, Chastain WH, Wang H, Ouvrier B, Bix GJ. Optimizing intraluminal monofilament model of ischemic stroke in middle-aged Sprague-Dawley rats. BMC Neuroscience. 2022; 23: 75. https://doi.org/10.1186/s12868-022-00764-2
[17] Rogers DC, Campbell CA, Stretton JL, Mackay KB. Correlation between motor impairment and infarct volume after permanent and transient middle cerebral artery occlusion in the rat. Stroke. 1997; 28: 2060–2065; discussion 2066. https://doi.org/10.1161/01.str.28.10.2060
[18] Longa EZ, Weinstein PR, Carlson S, Cummins R. Reversible middle cerebral artery occlusion without craniectomy in rats. Stroke. 1989; 20: 84–91. https://doi.org/10.1161/01.str.20.1.84
[19] Bederson JB, Pitts LH, Tsuji M, Nishimura MC, Davis RL, Bartkowski H. Rat middle cerebral artery occlusion: evaluation of the model and development of a neurologic examination. Stroke. 1986; 17: 472–476. https://doi.org/10.1161/01.str.17.3.472
[20] Qin C, Yang S, Chu YH, Zhang H, Pang XW, Chen L, et al. Signaling pathways involved in ischemic stroke: molecular mechanisms and therapeutic interventions. Signal Transduction and Targeted Therapy. 2022; 7: 215. https://doi.org/10.1038/s41392-022-01064-1
[21] Liu T, Li X, Zhou X, Chen W, Wen A, Liu M, et al. PI3K/AKT signaling and neuroprotection in ischemic stroke: molecular mechanisms and therapeutic perspectives. Neural Regeneration Research. 2025; 20: 2758–2775. https://doi.org/10.4103/NRR.NRR-D-24-00568
[22] Zhang P, He Y, Zhen Q, Zhang Y. Systematic Exploration of Potential Druggable Genes for Ischemic Stroke Employing Genome-Wide Mendelian Randomization Analysis. Brain and Behavior. 2025; 15: e70857. https://doi.org/10.1002/brb3.70857
[23] Levinson S, Pulli B, Heit JJ. Neuroinflammation and acute ischemic stroke: impact on translational research and clinical care. Frontiers in Surgery. 2025; 12: 1501359. https://doi.org/10.3389/fsurg.2025.1501359
[24] She R, Liu D, Liao J, Wang G, Ge J, Mei Z. Mitochondrial dysfunctions induce PANoptosis and ferroptosis in cerebral ischemia/reperfusion injury: from pathology to therapeutic potential. Frontiers in Cellular Neuroscience. 2023; 17: 1191629. https://doi.org/10.3389/fncel.2023.1191629
[25] Wang H, Li J, Zhang H, Wang M, Xiao L, Wang Y, et al. Regulation of microglia polarization after cerebral ischemia. Frontiers in Cellular Neuroscience. 2023; 17: 1182621. https://doi.org/10.3389/fncel.2023.1182621
[26] Semba S, Itoh N, Ito M, Harada M, Yamakawa M. The in vitro and in vivo effects of 2-(4-morpholinyl)-8-phenyl-chromone (LY294002), a specific inhibitor of phosphatidylinositol 3'-kinase, in human colon cancer cells. Clinical Cancer Research : an Official Journal of the American Association for Cancer Research. 2002; 8: 1957–1963.
[27] Walker EH, Pacold ME, Perisic O, Stephens L, Hawkins PT, Wymann MP, et al. Structural determinants of phosphoinositide 3-kinase inhibition by wortmannin, LY294002, quercetin, myricetin, and staurosporine. Molecular Cell. 2000; 6: 909–919. https://doi.org/10.1016/s1097-2765(05)00089-4
[28] O'Collins VE, Macleod MR, Donnan GA, Horky LL, Van Der Worp BH, Howells DW. 1,026 experimental treatments in acute stroke. Annals of Neurology. 2006; 59: 467–477. https://doi.org/10.1002/ana.20741
[29] Chamorro Á, Dirnagl U, Urra X, Planas AM. Neuroprotection in acute stroke: targeting excitotoxicity, oxidative and nitrosative stress, and inflammation. The Lancet. Neurology. 2016; 15: 869–881. https://doi.org/10.1016/S1474-4422(16)00114-9